NeuroImage: Clinical 30 (2021) 102609

Contents lists available at ScienceDirect

NeuroImage: Clinical

journal homepage: www.elsevier.com/locate/ynicl

The dynamics of theta-related pro-active control and response inhibition processes in AD(H)D

Nico Adelhöfer [1], Annet Bluschke [1], Veit Roessner, Christian Beste [*]

Cognitive Neurophysiology, Department of Child and Adolescent Psychiatry, Faculty of Medicine, TU Dresden, Germany

ARTICLE INFO

Keywords:
Attention deficit hyperactivity disorder
EEG
Theta
Response inhibition
Cognitive control

ABSTRACT

Impulsivity and deficits in response inhibition are hallmarks of attention-deficit(-hyperactivity) disorder (AD(H)D), can cause severe problems in daily functioning, and are thus of high clinical relevance. Traditionally, research to elucidate associated neural correlates has intensively, but also quite selectively examined mechanisms *during* response inhibition in various tasks. Doing so, in-between trial periods or periods prior to the response inhibition process, where no information relevant to inhibitory control is presented, have been neglected. Yet, these periods may nevertheless reveal relevant information. In the present study, using a case-control cross-sectional design, we take a more holistic approach, examining the inter-relation of pre-trial and within-trial periods in a Go/Nogo task with a focus on EEG theta band activity. Applying EEG beamforming methods, we show that the dynamics between pre-trial (pro-active) and within-trial (inhibition-related) control processes significantly differ between AD(H)D subtypes. We show that response inhibition, and differences between AD(H)D subtypes, exhibit distinct patterns of (at least) three factors: (i) strength of pre-trial (pro-active control) theta-band activity, (ii) the inter-relation of pro-active control and inhibition-relation theta band activity and (iii) the functional neuroanatomical region active during theta-related pro-active control processes. This multi-factorial pattern is captured by AD(H)D subtype clinical symptom clusters. The study provides a first hint that novel cognitive-neurophysiological facets of AD(H)D may be relevant to distinguish AD(H)D subtypes.

1. Introduction

Impulsivity and deficits in response inhibition are hallmarks of attention-deficit(-hyperactivity) disorder (AD(H)D), can cause severe problems in daily functioning, and are thus of high clinical relevance (Bari and Robbins, 2013; Chmielewski et al., 2018; Fallgatter et al., 2005, 2004; Paul-Jordanov et al., 2010; Pliszka et al., 2007; Seifert et al., 2003). Owing to this high clinical relevance, the neurophysiological (EEG) processes underlying response inhibition deficits in AD(H)D have been studied extensively (Albrecht et al., 2014; Baijot et al., 2017; Bluschke et al., 2016a; Doehnert et al., 2013; Fallgatter et al., 2004; Johnstone et al., 2009; Smith et al., 2004). In such studies, classical experimental approaches such as Go/Nogo and Stop-signal paradigms are used and the examination of neurophysiological processes is then focused on the time period after a certain stimulus has been presented (e.g. a Nogo or Stop stimulus); i.e. *during* response inhibition processes. Cognitive neuroscience studies in healthy populations suggest that theta-band activity is prominently involved in inhibitory control mechanisms triggered by such stimulus input (Chmielewski et al., 2016; De Blasio and Barry, 2013; Dippel et al., 2016, 2017; Huster et al., 2013; Isabella et al., 2015; Pscherer et al., 2019; Quetscher et al., 2015). In AD(H)D, alterations in theta band-related processes during inhibitory control have also been described (Pertermann et al., 2019; Yordanova et al., 2013) and are already targeted in interventions to ameliorate response inhibition deficits in AD(H)D (Bluschke et al., 2018). Yet, crucially, in-between trial periods or periods prior to the response inhibition process, where no information relevant to inhibitory control is presented, have been ignored in research on inhibitory control in AD(H)D, but may nevertheless reveal relevant information.

Interestingly, theta band activity is also important for pro-active control (Cooper et al., 2017, 2015) and thus for processes preparing the cognitive system to engage in a specific cognitive control subprocess (Braver, 2012), such as response inhibition. Although pro-active control-related theta band activity has mostly been examined after the

* Corresponding author at: Cognitive Neurophysiology, Faculty of Medicine Carl Gustav Carus, TU Dresden, Department of Child and Adolescent Psychiatry, Fetscherstrasse 74, 01307 Dresden, Germany.
E-mail address: christian.beste@uniklinikum-dresden.de (C. Beste).
[1] These authors contributed equally.

https://doi.org/10.1016/j.nicl.2021.102609
Received 20 May 2020; Received in revised form 7 February 2021; Accepted 17 February 2021
Available online 4 March 2021

presentation of "cues" that directly predict an upcoming event (Cooper et al., 2017, 2015; Cunillera et al., 2012; van Driel et al., 2015), it is possible that theta-band activity between trials is essential for the neural implementation of inhibitory control. This is because participants build expectancies about upcoming events and the likelihood of the need to engage in inhibitory control that persists across trials (Adelhöfer and Beste, 2019; Zavala et al., 2018). Moreover, some evidence indicates that pre-stimulus neurophysiological oscillations modulate cognitive control during inhibition (De Blasio and Barry, 2013; Smith et al., 2006). This sort of activity (i.e. pre-trial theta band activity; ptTBA) and its relation to inhibitory control-related theta band activity has, to the best of our knowledge, not been examined in AD(H)D thus far. It is the goal of the current study to examine this novel facet in the dynamics of inhibitory control in AD(H)D. Since pro-active control processes are essential for the implementation of inhibitory control (Hong et al., 2017; Liebrand et al., 2017; Randall and Smith, 2011; Smith et al., 2007; Vuillier et al., 2016), we hypothesize that the strength (evoked power) of ptTBA is correlated with the strength (evoked power) of theta band activity during response execution and inhibitory control within the trial (i.e. wtTBA). This hypothesis may seem trivial, but assumes that the "content" of the information in the ptTBA and the wtTBA are similar to a certain degree. However, although theta oscillations are associated with cognitive control in general, they have actually been shown to reflect different facets such as top-down attentional control, response inhibition, conflict/interference monitoring and working memory (Cavanagh and Frank, 2014; Cohen, 2014a; Hsieh and Ranganath, 2014; Jensen, 2006). Importantly, these aspects have been suggested to reflect relatively independent facets of cognitive control (Diamond, 2013; Miyake et al., 2000). However, a significant correlation between ptTBA and wtTBA would require that the type of information encoded in the pre-trial interval and during the trial is somehow associated or similar. Only if processes encoded in the theta band during the pre-trial interval have a high relevance for processes reflected in the theta band during the trial, the correlation would turn out to be relatively high and positive. Within a Go/Nogo task, participants are required to build across-trial expectancies about upcoming events and about the likelihood of the need to engage in inhibitory control (Adelhöfer and Beste, 2019; Zavala et al., 2018). Since working memory processes affect the unfolding of inhibitory control processes (Chmielewski et al., 2015), ptTBA can be hypothesized to represent inhibitory control-related working memory processes. Thus, ptTBA and wtTBA are thus presumably closely linked via inhibition-related processes, we hypothesize that a strong ptTBA is linearly correlated with wtTBA in that higher ptTBA is associated with stronger wtTBA.

However, a critical factor to consider in this hypothesized relationship between ptTBA and (inhibition-related) wtTBA in AD(H)D is that different AD(H)D subtypes have to be distinguished. The most important ones are the inattentive subtype (ADD) and the combined ADHD subtype (Ahmadi et al., 2014; Randall et al., 2009). Previous research suggests that these AD(H)D subtypes differ in their ability to inhibit responses as well as in the associated neurophysiological dynamics (Aldemir et al., 2018; Bluschke et al., 2016b; Kenemans et al., 2005). Thus, it is very important to consider the AD(H)D subtype when examining the dynamics between pro-active and inhibition-related theta band activity in children and adolescents with AD(H)D. It has been proposed that oscillatory dynamics may bear the potential to distinguish between AD(H)D subtypes (Aldemir et al., 2018). On that basis it is reasonable to hypothesize that the correlational pattern between ptTBA and wtTBA differs between AD(H)D subtypes. However, the precise pattern of subtype differences can, at present, not be deduced from current literature. It is possible that patients with different AD(H)D subtypes show a pattern in which the strength of correlation differs between them while the direction of the correlation is still the same. It is, however, also possible that patients with one subtype do not show correlations between ptTBA and wtTBA while those affected by the other subtype do. In any case, the dynamics of theta-related pro-active control and response inhibition processes will then represent a novel, clinically relevant metric to distinguish patients with different AD(H)D subtypes from each other.

To examine these questions, this study utilizes a sequential data analysis approach: In a first step, we analyze the relationship between pro-active and inhibition-related theta band activity regardless of AD(H)D subtype. In a second step, we examine the relevance of AD(H)D subtypes in more detail. For the data analysis, we use EEG data recorded from patients with AD(H)D and healthy controls in a standard Go/Nogo task. To examine theta dynamics of ptTBA and wtTBA, we first identify brain regions associated with both these forms of theta band activity using the dynamic imaging of coherent sources (DICS) beamforming approach (Gross et al., 2001). For these functional neuroanatomical sources, we reconstruct the time course of theta band activity using a linear constraint minimum variance beamforming approach (LCMV) (Dippel et al., 2017; Van Veen et al., 1997). This source-level time series data of ptTBA and wtTBA is then used to examine the above hypotheses. Further details are presented in the methods section. The reason why we perform the correlation analysis on the beamformed EEG data is that the applied beamforming methods (especially the LCMV beamforming step) reduce residual variance in the data (Dippel et al., 2017; Van Veen et al., 1997). The reduction of residual variance increases the reliability of the correlation analysis. Moreover, due to the spatial filter properties of beamforming (Gross et al., 2001; Handy, 2009), this approach circumvents the problem of spurious volume conduction effects that can also compromise the correlational results. Lastly, this approach also informs the functional neuroanatomical level, which is important to consider given that structure-functional biomarkers are important to develop in ADHD (Albajara Sáenz et al., 2019; Uddin et al., 2017). Since no clear-cut hypotheses can be deduced regarding the precise differential pattern of the relationship between ptTBA and wtTBA in different AD(H)D subtypes, data-driven methods (i.e. cluster analyses) are used to examine the pattern of correlations between ptTBA and wtTBA depending on AD(H)D subtype.

2. Materials and methods

2.1. Participants and patients

In a case-control cross-sectional study, we examined children/adolescent patients with AD(H)D compared to healthy controls. All participants included in the patient group had been diagnosed with AD(H)D in an outpatient clinic setting. Diagnoses were determined by a multi-professional team according to standard clinical guidelines. These include family and teacher interviews, symptom questionnaires (see below), IQ (WISC-IV) and attention testing. Further, possible underlying somatic disorders were checked for using EEG, blood analyses and hearing and vision tests. After diagnoses had been confirmed, patient families were contacted by telephone to enquire whether they were interested in participating in this study. N = 47 subjects (10 female) agreed to participate in this study (N = 28 medicated with methylphenidate (extended release)). N = 22 had been clinically diagnosed with ADD (ICD-10: F98.8), while N = 25 were clinically diagnosed with the combined subtype (ADHD; ICD-10 F90.0 or F90.1). None of the patients suffered from any psychiatric comorbidities like tic/Tourette, autism spectrum disorders, depression, conduct or oppositional defiant disorder. Two patients had additionally received a diagnosis of adjustment disorder, while three had a confirmed Axis II diagnosis (n = 2 with developmental coordination disorder, n = 1 with dyslexia). Due to the recruitment context (outpatient clinic setting), it was not feasible to record the number of participants who were not interested or able to take part in the study.

We further recruited a sample of healthy controls (N = 50, 21 female) from our in-house database and by external advertisements. AD(H)D had been excluded in this control sample by means of a telephone interview concerning ICD-10 diagnostic criteria for AD(H)D. In case of

good suitability for the study, questionnaires were sent to the families beforehand, which were filled out at home (see below). These questionnaires were also used to confirm that no AD(H)D symptoms were reported by parents or children. Any items that had been marked by the parents as applicable to their child were discussed with the families at the start of the research appointment. Participants were excluded from the study if symptoms of severe or acute psychiatric disorders were reported during the initial telephone screening or in the questionnaires (except for AD(H)D in the patient group). They were also not included in the study if the IQ score was below 85 points (as assessed by a short form of WISC-IV; (Waldmann, 2008)), were outside of the required age range of 8–15 years, or had performed the Go/Nogo task before. Please refer to Table 1 for demographic information.

The questionnaire "AD(H)D Symptom Checklist" from the DISYPS II (Döpfner et al., 2008) was completed by parents. Parents scored their children on a scale of 0 (no problems) to 3 (severe problems) for core AD (H)D symptoms (Table 1). Average values above 1.5 suggest that symptoms are clinically severe (Döpfner et al., 2008). Healthy controls scored significantly lower than the patient group on all three subscales (all $F \geq 101.75$; $p \leq 0.001$; $\eta_p^2 \geq 0.525$). Patients with ADD and ADHD displayed a similar degree of inattentive symptoms ($p = 282$). As expected, patients with ADHD displayed significantly stronger hyperactive ($p \leq 0.001$) and impulsive ($p \leq 0.001$) symptoms. Groups did not differ in age or IQ (both $F \leq 0.46$; $p \geq 0.631$; $\eta_p^2 \leq 0.010$) (see Table 1). Overall, the number of included participants was even slightly larger than it was the case in previous studies using the same experimental paradigm (Bluschke et al., 2016b, 2018, 2020), justifying the assumption of this study being sufficiently powered. Due to the novel and complex analysis approach applied to the EEG data, it was not possible to conduct a separate power analysis for this data.

Written informed consent was obtained from all participants or their legal guardians. The study was approved by the ethics committee of the TU Dresden.

2.2. Task

A Go/Nogo task was used to examine inhibition performance (Beste et al., 2011; Chmielewski et al., 2015). Within this task, the word 'DRÜCK' (German for 'PRESS'; Go stimulus) or 'STOP' (Nogo stimulus) was presented for 300 ms in white font on a black background. In case of a Go stimulus, participants were required to perform a button press with the right index finger within 500 ms. The participants had to refrain from reacting when a 'STOP' stimulus was presented. The intertrial interval was jittered between 1600 ms and 1800 ms. The experiment consisted of 248 Go experiments and 112 Nogo trials which were presented in a pseudo-randomized order. The task lasted about 20 min. Before the start of the experiment, participants familiarized themselves with the task completing 18 practice trials (6 Nogo trials; pseudo-randomized order).

2.3. EEG recording and analysis

EEG was recorded using an equidistant electrode setup of 60 Ag/AgCl electrodes with a sampling rate of 500 Hz (reference at Fpz, the ground electrode at $\theta = 58$, $\phi = 78$) using a QuickAmp amplifier (Brain Products Inc.) and the Brain Vision Recorder software (Brain Products Inc.). Offline data processing was carried out as already described in Adelhöfer et al. (2018): recorded data was down-sampled to 256 Hz and a bandpass filter (0.5–20 Hz, IIR zero phase Butterworth, slope: 48 dB/oct.) was applied. Technical artefacts were identified by visual inspection in the raw EEG data. An independent component analysis was then used to detect and remove periodically occurring artefacts (e.g., pulse artefacts, horizontal and vertical eye movements). The data was segmented to the onset of the Go and Nogo stimuli (-1000 ms before stimulus onset to 1500 ms after stimulus onset). Only trials with correct responses to Go stimuli and without responses to Nogo stimuli were analyzed further. Remaining artefacts were removed by an automatic artefact rejection procedure (amplitude criterion: maximum amplitude: +200 μV, minimum amplitude: −200 μV; maximum value criterion: a difference of max. 200 μV in an interval of 200 ms; low activity criterion: activity below 0.5 μV in a period of 100 ms). The remaining trials in each group were for ADD: 190 ± 31 Go, 46 ± 23 Nogo; for ADHD: 202 ± 31 Go, 60 ± 21 Nogo; for controls: 212 ± 28 Go, 71 ± 19 Nogo. Importantly, a statistical analysis of these frequencies using the factor Go/Nogo and group revealed no interaction "Go/Nogo × group (ADHD, ADD, controls)" ($F(2,94) = 0.19$; $p = 0.828$). This lack of interaction that there are no systematic differences in the frequencies of trials used for the EEG data analysis. This shows that differences obtained at the EEG level (cf. results section) are not due to systematic differences in trial numbers constituting an important factor for the SNR of the obtained data and reliability of the results.

These single-trial segments were then averaged for each condition, which served as the basis for the following time–frequency analyses using Morlet wavelets (w). Given the input parameters time (t) and frequency (f), the wavelets were defined as

$$w(t,f) = A\exp\left(-\frac{t^2}{2\delta_t^2}\right)\exp(2i\pi ft)$$

The remaining parameters are defined as $A = (\delta_t\sqrt{\pi})^{-1/2}$, δ_t: wavelet duration and $i = \sqrt{-1}$. We used $f_0/\delta_f = 5$ with f_0 being central frequency and δ_f the width of the Gaussian shape in the frequency domain. As the basis for the next analysis steps, we used the power between frequencies 4 to 7 Hz (theta band) in the single-trial EEG data. To test whether there were statistically significant clusters of electrodes exhibiting theta-band activity, we employed a method similar to cluster-based permutation tests from the FieldTrip toolbox (Maris and Oostenveld, 2007). Different from cluster-based permutation tests, we did not contrast two experimental conditions, but each condition against a baseline array containing only zeros (i.e. hypothetically non-existent theta-band power). That is, we adjusted functions from the FieldTrip toolbox as follows: For the reference distribution, trials (including those containing only zeros) were randomly assigned to either the experimental condition or the baseline (1000 randomizations). The largest electrode cluster was identified based on this random categorization. The frequency distribution of the randomly assigned clusters served as the reference distribution, and clusters exceeding the largest 5% of the reference distribution (i.e. the largest sum of t values for all electrodes in this cluster) were considered significant. Resulting clusters are shown as inlays in Fig. 2 for each condition (all $p < 0.001$).

2.4. Beamforming-based source localization analysis

As mentioned in the introduction, theta source activity was reconstructed in a two-step approach (Dippel et al., 2017). First, we employed dynamic imaging of coherent sources beamformer (DICS) (Gross et al., 2001). We used Fieldtrip functions (Oostenveld et al., 2003) to derive power values for each source voxel using DICS. For that, we first performed a spectral analysis with a multitaper frequency transformation and obtained the cross-spectral density matrix. Since the theta band is defined from 4 to 7 Hz, we set the centre frequency to the frequency

Table 1
Demographical Information. No significant differences between groups and subgroups were evident ($p \geq 0.631$).

	Controls	AD(H)D Patients	
		ADD	ADHD
Age	11.4 (±2.0)	11.9 (±2.2)	
		11.8 (±2.1)	12.0 (±2.2)
IQ	107.5 (±12.4)	106.3 (±11.6)	
		105.2 (±12.1)	107.3 (±11.3)

band's centre at 5.5 Hz and used a smoothing window of ±1.5 Hz. We used an MNI brain template included in Fieldtrip as the forward model. It consists of a grid of 6 mm voxels in each dimension. After the realignment of the employed EEG electrodes to the forward model, a leadfield matrix was computed by partitioning the forward model's brain volume into a grid with 6 mm resolution. For every voxel and using the realigned EEG channel positions based on the template, the voxel leadfield matrices were computed. In addition, the cross-spectral density matrix was computed. Based on this, a common spatial filter (regularization parameter set to 5%) was derived. Applying this filter yielded the source power of the grid coordinates in the theta frequency band and the time windows of interest. Regarding the latter, we defined two time windows were chosen for DICS beamforming, representing the pre-trial and within-trial condition, respectively. The duration of both time windows was set to 800 ms in order to ensure at least 3 full cycles in the theta range to obtain reliable theta power estimations. The 800 ms time windows either ended at the stimulus onset for the pre-trial phase (i.e. for ptTBA) or started at the stimulus onset for the wtTBA analysis. Since noise in the data usually shows with a maximum towards the centre of the head model, relevant neural activity can be obscured if only raw power values are investigated (Van Veen et al., 1997). Therefore, we divided power values by the respective local noise estimates. These values, which vary as a function of location, were derived using implemented functions in Fieldtrip (Maris and Oostenveld, 2007) based on the smallest eigenvalue of the cross-spectral density matrix. This normalization procedure yielded the Neural Activity Index (NAI), which provides estimates of source neural activity. Please note that the number of channels in this study is sufficient to provide reliable localization results, as could be shown recently based on a combined simulation/empirical approach (Halder et al., 2019). In this study, authors found that high localization accuracy can be achieved from DICS and LCMV beamforming approaches, given a similar amount of sensors and provided that the signal-to-noise ratio (SNR) of the data is sufficiently high. We could ensure a high SNR via impedance control of the electrodes prior to the task. Regarding the further beamforming analyses (see below), only the voxel with maximum NAI power (based on Grand Average data) was selected. Since we did not focus on the full extent of a source voxel cluster, but rather a central voxel with highest activity, the likelihood that the source is located within a task-relevant anatomical region is further increased.

2.5. Statistical analysis

Task-related effects and effects of the different patient groups/participants were analyzed using parametric tests (ANOVAs and t-tests). The main focus, however, was on the correlational analysis based one LCMV beamforming analysis (Van Veen et al., 1997) applied to the results of the DICS analysis. The LCMV analysis reveals the time course of theta band activity in each DICS-reconstructed source of the NAI (Dippel et al., 2017; Van Veen et al., 1997). For the LCMV analysis, as implemented in the Fieldtrip toolbox (Maris and Oostenveld, 2007), the covariance matrix was calculated. Using this matrix, and the previously identified voxels from the DICS beamforming step, the adaptive spatial filter of the LCMV beamformer was calculated. We obtained the single-trial time series of the reconstructed source by multiplying the spatial filter with the preprocessed EEG data. These time series at source level were then decomposed to time–frequency data for each trial (see above). Theta band oscillations were then averaged and isolated (4–7 Hz). Next, the theta oscillatory activity of the individual trial level was averaged. This resulted in the theta band time series at the source level for ptTBA and wtTBA, which were used for the correlation analyses of the ptTBA and wtTBA time series data:

Pearson correlations were computed between every time point of the ptTBA time series and the wtTBA time series within each group of participants included in the study (i.e. controls and both groups of AD(H)D patients) and Go or Nogo trials. This results in a matrix of group correlation coefficients with the axes pre-trial interval time course (y-axis) and within-trial interval time course (x-axis). Crucially, for the statistical analysis, it is required that an estimate of the correlation coefficient is evident for each individual and not only at the group level. Although individual correlation values can be obtained using single-trial data, this approach might bias into correlation coefficients, because trial numbers vary across participants and conditions. More important, however, single trial EEG data are inherently noisy, which limits interpretability of the resulting correlations. For this reason, we derived these individual subject estimates of the correlation between ptTBA and wtTBA based on average values by employing a jack-knife procedure (Miller et al., 1998), as introduced recently (Adelhöfer and Beste, 2020): To obtain the jackknifed correlation coefficients (i.e. coefficients for the single subjects), correlation analyses are calculated across participants by successively omitting data from every participant once. This results in n jack-knifed correlations ($j \ldots j_n$), with each j_i being based on the data from all participants but i. These jack-knife analyses were conducted for each group and condition, separately. These single-subject correlation coefficient data were then used in further analyses. For the statistical analysis, we focused on the mean single-subject correlation coefficient between the time ranges −800 to 0 ms (i.e. the ptTBA) and the analyzed time interval in the trial data (wtTBA; 200 ms to 450 ms after stimulus onset). The duration of 800 ms ensured that the ptTBA interval did not overlap with the stimulus–response interval of the previous trial. This was the case for any participant and trial. The wtTBA interval was chosen upon visual inspection of source theta activity (see Fig. 2) and various previous findings using the same task suggesting that theta activity during response inhibition is strongest in this time window (Beste et al., 2011; Quetscher et al., 2015). Prior to the statistical analysis, all these single-subject mean correlation coefficients were Fisher Z-transformed to achieve a normal distribution of the data (Gayen, 1951). Note that because of this transformation, correlation coefficients are not bound between −1 and 1. Since the application of the jack-knifing procedure reduces variance in the data, this artificial reduction in variance needs to be corrected in the statistical analyses. For that, we applied the correction procedure by (Ulrich and Miller, 2001). These corrected F-values are denoted as F_{corr}.

3. Results

3.1. Behavioral data

The behavioral data results are shown in Fig. 1.

For Go trials, we found no significant reaction time (RT) difference between the patients with AD(H)D (466 ± 18 ms) and the control group (458 ± 14 ms) ($t(95) = 0.34$; $p = 0.736$; $d = 0.068$). Also, rates of correct responses did not differ significantly between the two groups ($t(95) = 1.11$; $p = 0.271$; $d = 0.226$; patients: 95.9 ± 0.6%; controls: 97.0 ± 0.8%). False alarm rates (i.e. responses in Nogo trials) differed between the groups ($t(95) = 3.76$; $p < 0.001$; $d = 0.761$). False alarm rates in the patient group were higher (45.0 ± 3.7%) than in the control group (28.0 ± 2.6%).

3.2. Neurophysiological data

The time–frequency data for each trial type and group are displayed in Fig. 2. Mean sensor-level and source-activity waveforms (±SD) for the theta-band response (4–7 Hz) over time are given in Supplementary Figs. 1 and 2. In Fig. 2, the left-hand plots denote activity in the pre-trial interval (ptTBA, i.e. before Go or Nogo stimulus onset, respectively) while the right-hand plots denote activity within the trial (wtTBA, i.e. after Go or Nogo stimulus onset).

Regarding ptTBA, we did not observe a significant effect of group ($t(95) = 1.28$; $p = 0.202$; $d = 0.260$; control group: 2.94 ± 0.01 μV^2; patient group: 2.72 ± 0.14 μV^2). ptTBA was not supposed to differ between Go and Nogo trials, since the likelihood of any trial type was

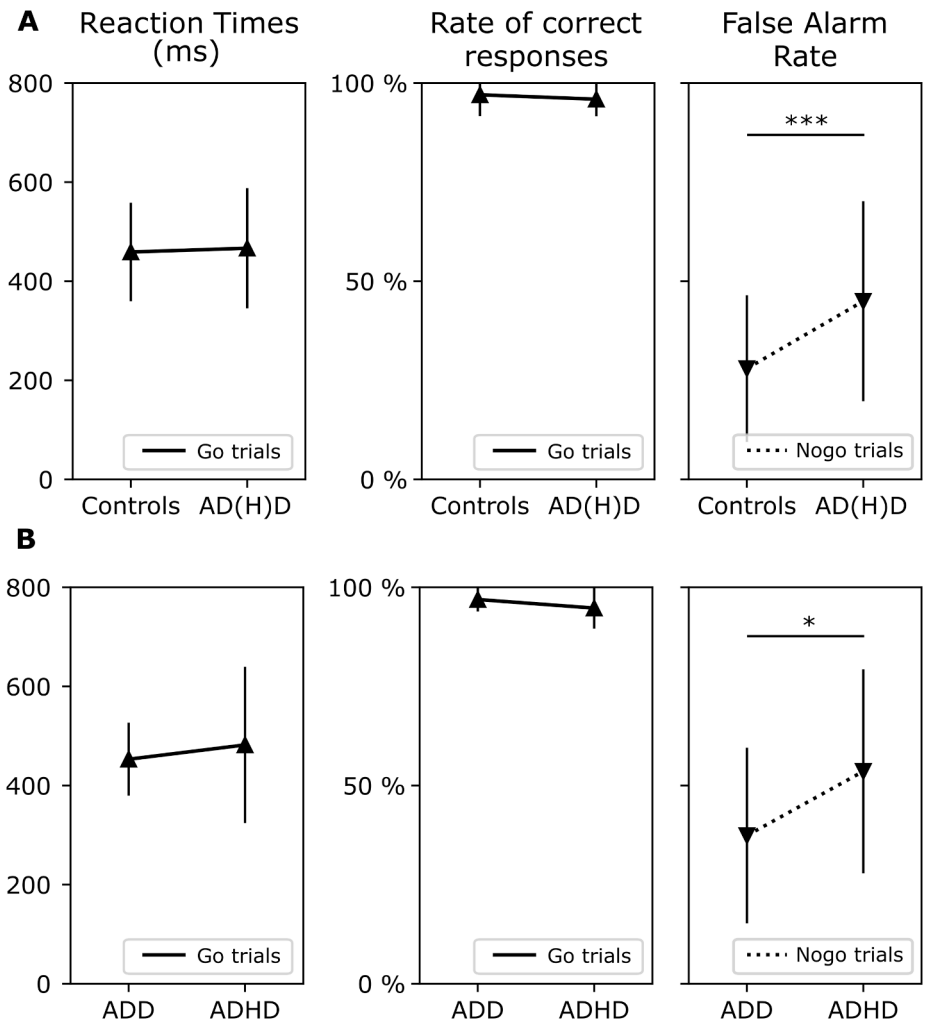

Fig. 1. *Depiction of behavioural data.* Part A shows the comparison between controls and the AD(H)D group. Part B shows the comparison between the ADD and the ADHD group. Reaction time (left panel), rate of correct responses (central panel) and false alarm rate data (right panel) are shown. The triangles indicate the means, vertical lines represent standard deviations. Both parameters are shown separately for healthy controls (N = 50) and AD(H)D-diagnosed subjects (N = 47; top row) as well as for ADD (N = 22) and ADHD-diagnosed subjects (N = 25; bottom row; see x-axes).

constant over the whole experiment, which means that likelihoods were independent of the type of the upcoming trial. Therefore, preparatory activity should not be different regarding the upcoming trial type (Go vs. Nogo). This is confirmed by a within-sample *t*-test of pretrial theta power between Go and Nogo trials ($t(96) = 0.54$; $p = 0.590$).

For the wtTBA a main effect trial type is shown ($F(1,95) = 20.83$; $p < 0.001$; $\eta_p^2 = 0.180$). There was a higher TBA in Nogo trials (2.90 ± 0.07 μV^2) than Go trials (2.58 ± 0.08 μV^2). The main effect group was not significant ($F(1,95) = 0.23$; $p = 0.634$; $\eta_p^2 = 0.002$). Also, no interaction effect between group and trial type was detected ($F(1,95) = 1.83$; $p = 0.179$; $\eta_p^2 = 0.019$).

In the next step, we examined whether the degree of ptTBA was correlated with wtTBA and whether these correlations are modulated by trial type and/or group. Fig. 3 shows the results of these analyses. Table 2 displays the respective anatomical regions and coordinates identified via DICS beamforming for control and patient group.

The top row in Fig. 3 shows the voxel locations in the standard MNI brain that were identified via beamforming analysis. Data are shown for controls and patients with AD(H)D, in Go and Nogo trials. For Go and Nogo trials, the source of ptTBA is shown on the left and the source of wtTBA shown on the right. As outlined in the methods, the time series of the theta source activity was extracted using LCMV beamforming and used for the correlation analysis; i.e. the time series in the pre-trial interval (ptTBA) was correlated with the time series in the post-stimulus interval (wtTBA). The results of these correlation analyses are shown in the lower row of Fig. 3. In these plots, the y-axis denotes the pre-trial interval and the x-axis the post-stimulus interval. The strength of correlations is colour coded. The statistical analysis, however, revealed that there were no significant differences in pre-trial/post-trial correlations of theta band activity. None of the included factors (main or interaction effects) in the ANOVA were significant (all $F_c \leq 1.74$, $p \geq 0.191$). Thus, there were no trial-dependent, group-dependent or trial x group dependent modulations of the correlation between ptTBA and wtTBA. However, the obtained correlation coefficients were rather low (see Fig. 3B), which indicates that the shape of scatterplot denoting the inter-relation between ptTBA and wtTBA in the control and ADHD sample is circular-shaped. Indeed, this is the case when inspecting the scatterplot for the healthy control group in Go and Nogo trials (see Fig. 4A left panel).

However, a close look at the data pattern (scatterplots) showing the correlations between ptTBA and wtTBA for Go trials (top row) and Nogo trials (bottom row) for the ADHD group suggest that there is not a homogenous distribution of the data in the scatterplot as it is the case for the control sample. Opposed to the control group, the regression line for the AD(H)D group is placed between the apparent data clusters (see Fig. 4). From the visual inspection of the data distribution shown in Fig. 4 it is clear that the linear correlation does not well capture the pattern/distribution of the individual data points. Rather, the distribution of the correlation coefficients between ptTBA and wtTBA falls apart in two clusters in the AD(H)D group. Especially for the Nogo trials, it seems that there are two distinct clusters (see Fig. 4A, middle panel). Therefore, there are further aspects in the data that need to addressed statistically. To test the possibility that there are indeed two distinguishable clusters in the AD(H)D sample, we performed a cluster

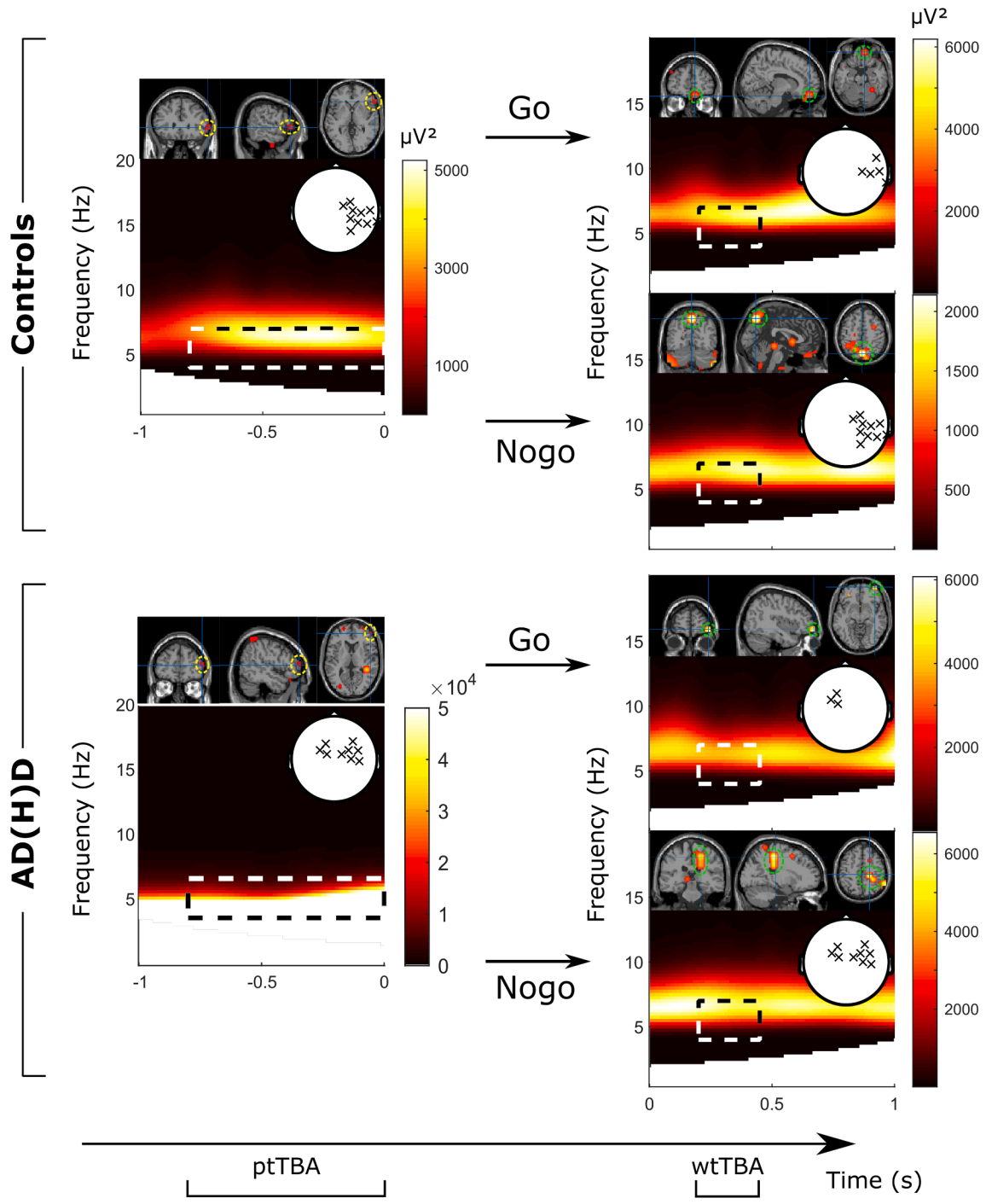

Fig. 2. *Average time–frequency EEG data* (i.e., *spectral power as a function of time point (x-axes) and frequency (y-axes))*. The figures show the groups (healthy controls vs. AD(H)D patients), trial types (Go vs. Nogo trials), and time intervals (pre-trial: left-hand side; within-trial: right-hand side). For each time–frequency plot, significant theta activity has been shown using cluster-based permutation tests. Significant electrodes are shown in the scalp topography plots. Also, the significant activation of functional neuroanatomical regions (i.e. theta source activity) is shown in the coronal, horizontal and sagittal slice views. Note that for pretrial activity (ptTBA, left-hand side), no distinction was made between Go and Nogo trials because participants could not predict whether the upcoming trial would be a Go or a Nogo trial. Dashed rectangular boxes show the time × frequency area which was used for source reconstruction. We analyzed the theta band (4 to 7 Hz) in all conditions and time ranges between −800 and 0 ms (pre-trial theta activity; ptTBA) and between 200 and 450 ms (within-trial theta activity; wtTBA). Time values are relative to stimulus onset. Precise locations of the neuroanatomical regions are shown in Table 2.

analysis. At this point it is important to mention that the performed cluster-analysis is not a sort of a post-hoc analysis of the ANOVA results since the cluster analysis captures different aspects in the data, to which the (standardized) correlations coefficient and ANOVAs are blind. The cluster analysis is able to capture the structure of the data (pattern of the individual data points in the scatterplot determining the strength of correlation), which was not possible in the ANOVA. Prior to running the cluster analysis, the mean theta band power values of every single participant were $\log_{10}$-transformed to achieve normal distribution of the data. For the cluster analysis, we employed the Gaussian mixture model (GMM) as implemented in Matlab (Johannes, 2020). This algorithm requires the number of expected clusters as input and provides the

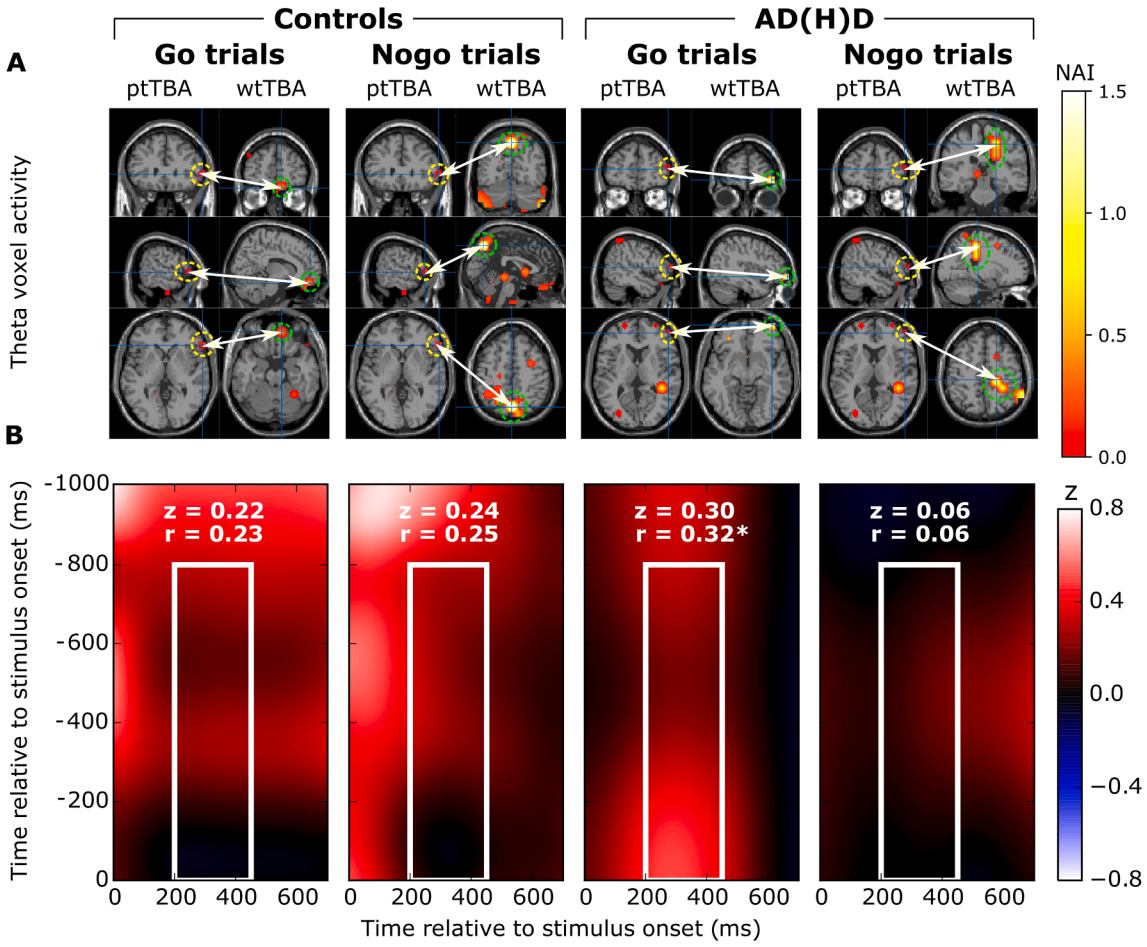

Fig. 3. *Main results of correlation analysis.* (A) Relevant anatomical sources (detailed in Table 2) for each condition as selected via DICS beamforming analysis of the neural activity index (NAI; details in text). White arrows indicate the regions used for the correlation analysis between ptTBA and wtTBA. Dashed circular lines additionally highlight the found neuroanatomical region. The colour scale shows the strength of activity (B) Mean correlations as a function of pretrial time (y-axes) and within-trial time sample (x-axes). Rectangular boxes display the time range used to calculate the means, which were then used for statistical analyses. We applied a Fisher Z-transformation prior to the Pearson correlations prior to statistical analyses. Correlation coefficients (r) and Z-values are shown. The colour scale shows the strength of correlations.

Table 2
Description of source regions identified with DICS beamforming.

		MNI label Controls	MNI coordinates (x,y,z)	Brodman Area
ptTBA		rIFG	6.0 | 2.9 | 0.0	BA45
wtTBA	Go	Rectus R	1.0 | 5.1 | −2.2	BA11
	Nogo	Precuneus	0.0 | −7.1 | 5.0	BA7
		AD(H)D patients		
ptTBA		Frontal Mid R	5.0 | 4.9 | 0.8	BA10
wtTBA	Go	Frontal Mid Orb R	4.0 | 5.9 | −1.0	BA10
	Nogo	Cingulum Mid R	1.6 | −2.7 | 4.8	BA6

pre-trial theta-band activity (ptTBA); within-trial theta-band activity (wtTBA)

probability of belonging to one of the clusters. Based on the visual inspection of the data distribution in the ADHD sample, the number of expected clusters was two and this may potentially reflect the AD(H)D subgroups. Since the result of the cluster analysis depends on the initial configuration of Gaussian parameters, we ran the algorithm 10-times and selected the resulting pattern with the most distinct clustering. The GMM revealed two significant clusters (Fig. 4A, right-most panel) for Go trials ($\chi^2 = 14.15$; $p < 0.001$) and two clusters for Nogo trials ($\chi^2 = 14.15$; $p < 0.001$). Note that χ^2 values are the same for Go and Nogo trials since cluster membership was independent of trial type. When labelling the clustered data points it become apparent that these two clusters refer to different AD(H)D subtypes. The ADD group is shown in blue and the ADHD group is shown in red. For Go and Nogo trials, one cluster predominantly represents ADD patients, the other cluster predominantly represents ADHD patients. Importantly, the obtained cluster results were only found for AD(H)D subtypes, but not when using IQ ($\chi^2 = 0.31$; $p = 0.579$) or age ($\chi^2 = 0.51$; $p = 0.474$) as a clustering criterion. Furthermore, no significant association was found between the obtained clusters and "medication status" ($\chi^2 = 1.33$; $p = 0.250$). As can be seen in Fig. 4A, the clustering result is largely (although not entirely) due to a separation in pre-trial theta power. This is corroborated by statistical analysis: As expected, the clusters differ significantly regarding ptTBA ($t(45) = 15.28$; $p < 0.001$). The results of the cluster analysis point to an aspect in the data that has not been captured when running the analysis over the entire groups of subjects. The results of the cluster analysis provide methodological/statistical justification to (re-)run the analyses on the inter-relation between ptTBA and wtTBA with specific focus on the statistically derived AD(H)D subgroup clusters. As can be seen in Fig. 4 (middle panel), not every patient that was clinically diagnosed with ADD or ADHD was part of the statistically derived ADD or ADHD cluster. For example, 3 patients with a clinical ADHD diagnosis were actually located in the cluster where the majority of patients with a clinical ADD diagnosis were collated. Therefore, the analyses conducted using the cluster information do not 1:1 relate to the clinical diagnosed group. The analyses steps undertaken after conducting the cluster

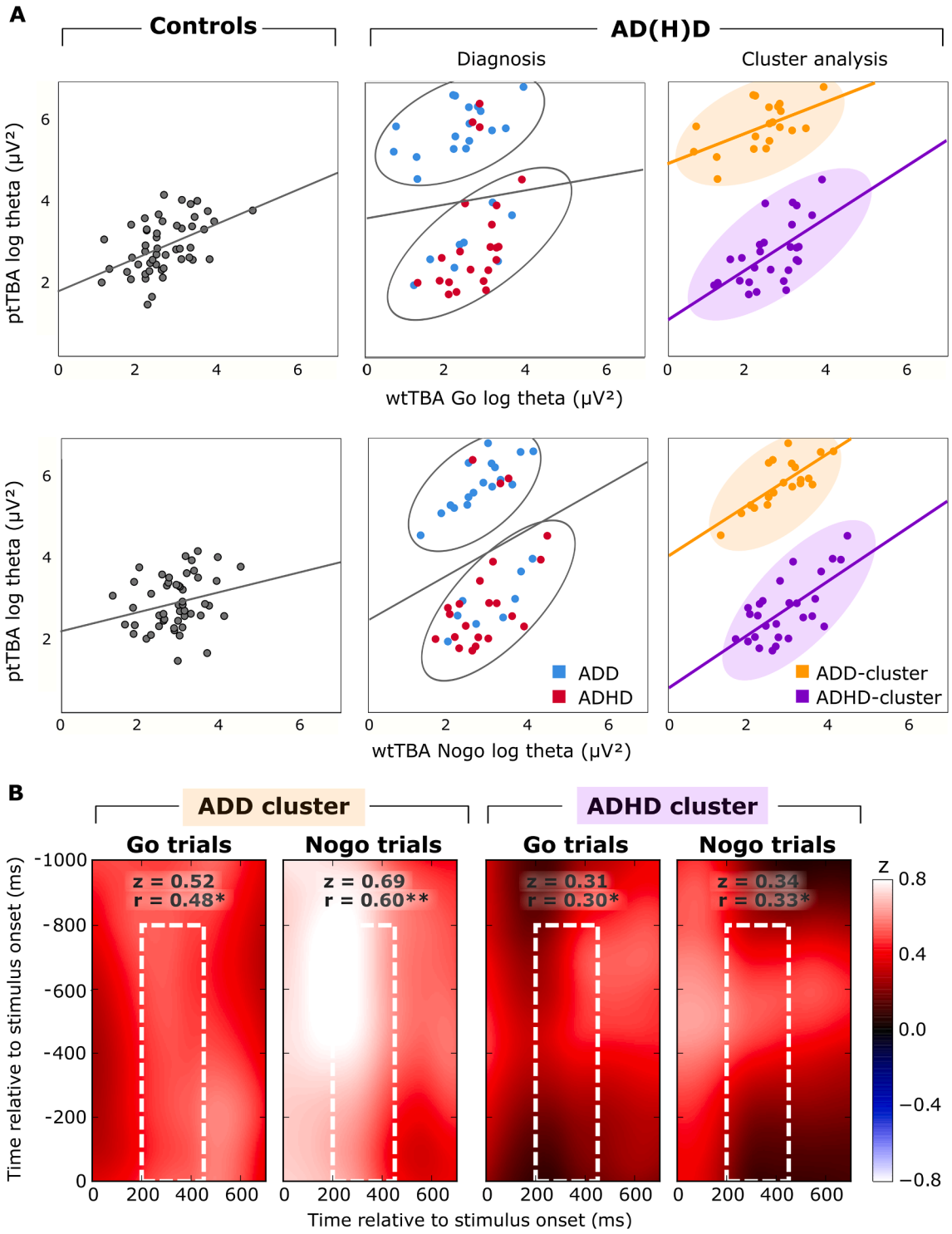

Fig. 4. *Results from correlations on the basis of the cluster analysis.* (A) Scatter plots showing the correlation of $\log_{10}$-transformed theta power between the pretrial interval (ptTBA) and the post-stimulus interval (wtTBA) for Go stimuli (top row) and Nogo stimuli (bottom row). Left panels: The data of the healthy group is shown with the regression line in grey. Middle panel: The correlation is shown in the ADHD sample with the regression line in grey. Two clearly distinct cluster can be seen. Patients belonging to the ADD group (as defined by the clinical diagnosis) are shown in blue, patients belonging to the ADHD group (as defined by the clinical diagnosis) are shown in red. It can be seen that the regression line is placed between the two clusters. Right panels: After the cluster analysis two distinct clusters can be defined and statistically verified. The orange cluster shows the ADD-cluster (as defined by the statistical cluster analysis), the purple cluster shows the ADHD-cluster (as defined by the statistical cluster analysis). The regression line is fit to each of the estimated clusters showing a clear positive correlation. (B) Results of correlation analysis with the ADD/ADHD subgroups as defined by the results from the cluster analysis. Figures show mean correlations as a function of pretrial time sample (y-axes) and within-trial time sample (x-axes). Rectangular boxes display the time area used to calculate grand means, which were then used for statistical analyses. We applied a Fisher Z-transformation prior to the Pearson correlations prior to statistical analyses. Correlation coefficients (r) and Z-values are shown. The colour scale shows the strength of correlations. (For interpretation of the references to colour in this figure legend, the reader is referred to the web version of this article.)

analysis were based on the statistically *estimated clusters of patients* and not using the already available clinical information diagnosing a patient as ADD or ADHD. When referring to ADD and ADHD in the forthcoming we relate to the statistically derived ADD/ADHD-clusters and not to the clinical diagnosis:

For ptTBA, we found a highly significant difference between the ADD cluster (5.87 ± 0.61 μV^2) and the ADHD cluster (2.62 ± 0.80 μV^2) ($t(45) = 15.91$; $p < 0.001$; $d = 4.60$). Regarding wtTBA, we only found a main effect of trial type ($F(1,45) = 18.08$; $p < 0.001$; $\eta_p^2 = 0.287$; Nogos: 2.88 ± 0.11 μV^2; Gos: 2.45 ± 0.11 μV^2), but no main effect of cluster ($F(1,45) = 0.61$; $p = 0.438$; $\eta_p^2 = 0.013$; ADD: 2.59 ± 0.15 μV^2; ADHD: 2.75 ± 0.13 μV^2) and no significant interaction effect ($F(1,45) = 0.85$; $p = 0.363$; $\eta_p^2 = 0.018$). Also, the correlations between ptTBA and wtTBA were tested again. The results are shown in Fig. 4B. All correlations were statistically significant. Specifically, there were positive correlations between ptTBA and wtTBA in Go trials ($r = 0.597$; $p = 0.005$) and Nogo trials ($r = 0.645$; $p = 0.002$) in the ADD cluster, as well as in Go trials ($r = 0.631$; $p < 0.001$) and Nogo trials ($r = 0.424$; $p = 0.028$) in the ADHD cluster. There were no significant differences in correlations regarding group-cluster, trial type or an interactive effect of both (all $F_c \leq 0.87$, $p \geq 0.357$).

In the last step, we examined how far the inter-relation between ptTBA and wtTBA affects behavioural performance in response inhibition (i.e. the rate of false alarms). Prior to computing these correlations, false alarm rates were Fisher's Z-transformed, upon which Pearson correlations were computed. The results are summarized in Table 3.

Since the control group did not show a significant correlation between ptTBA and wtTBA, co-variation between ptTBA-wtTBA correlations and false alarm rates in the control group cannot be meaningfully interpreted. Therefore, this group was not considered further to examine the relevance of the ptTBA-wtTBA inter-relation for behavioural performance. In the ADD group and the ADD cluster, showing better response inhibition performance than the ADHD group/cluster, no correlations were evident (see Table 3). In the ADHD group and the ADHD cluster, showing worst response inhibition performance, a stronger correlation between ptTBA and wtTBA in Nogo trials was correlated with a higher rate of false alarms (see Table 3). A scatterplot showing the correlation between the ptTBA/wtTBA correlation and rate of false alarms is given in supplemental Fig. 3.

4. Discussion

In this study, we investigated the interrelation of neural dynamics underlying pro-active control and inhibitory control processes in AD(H)D with special emphasis on differences between AD(H)D subtypes. We provide the first in-depth insights into the dynamics of pre-trial and within-trial periods in AD(H)D and its clinical relevance as a novel parameter which may be used to distinguish patients with ADHD and ADD from each other. Doing so, we use a previously published methodological approach developed using a healthy adult sample in related but not identical experimental paradigm (Adelhöfer and Beste, 2020).

The behavioural data revealed the typical response inhibition deficits in AD(H)D, i.e. an increase in false alarms relative to healthy controls (Kolodny et al., 2020; Metin et al., 2012; Pievsky and McGrath, 2018), and worse response inhibition performance in the ADHD group than the ADD group (Bluschke et al., 2016b). The analysis of source-level theta band activity showed that theta power was stronger during trials requiring response inhibition than in those requiring response execution. This is also well in line with the literature (Adelhöfer et al., 2019; Chmielewski et al., 2016; Hong et al., 2020; Nigbur et al., 2011; Yamanaka and Yamamoto, 2010; Zavala et al., 2018). We could show that different prefrontal cortical regions are associated with pro-active control theta dynamics (ptTBA) in healthy participants and patients with AD(H)D (see Table 2). The same was the case for theta dynamics underlying response execution and inhibition (wtTBA). Most important is the data on the dynamics between ptTBA and wtTBA associated with these functional neuroanatomical regions:

There was no correlation (inter-relation) between ptTBA and wtTBA in controls, suggesting that theta band dynamics during response execution and inhibition are largely decoupled from pro-active control dynamics occurring beforehand in the same frequency band. The same was the case in patients with AD(H)D. However, the data analysis showed that there was not a homogenous distribution of the data in the scatterplot denoting the inter-relation of ptTBA and wtTBA. This was confirmed by a cluster analysis. The cluster analysis shows that there were two distinct clusters, which further analyses showed can be labelled as an ADHD-cluster and an ADD-cluster. When performing analyses of the ptTBA and wtTBA inter-relation for these statistically derived clusters, the pattern of results changed (see Fig. 4). In both AD(H)D subtypes and for Go and Nogo trials, high ptTBA was associated with high wtTBA. This suggests that opposed to controls, theta band activity prior to the presentation of behaviourally relevant information (i.e. Go or Nogo stimuli) is strongly associated with neurophysiological processes occurring during behavioural control (i.e. response execution or inhibition) in an AD(H)D-subtype specific manner. This shows that in the case of AD(H)D-cluster, the neurophysiological processes during response inhibition and execution are less flexibly modulated and more dependent on the pre-existing level of neuronal activity. Importantly, the inter-relation (correlation) between ptTBA and wtTBA creates two distinct clusters that distinguish the ADD and the ADHD group very well. Thus, the inter-relation of pro-active control theta band activity and control-related theta band activity is a clinically useful metric to distinguish patients with ADD and ADHD. Further data analyses corroborated the robustness of this clustering since potential confounding factors like IQ, age or medication status did not allow for a similar clustering. Crucially, the obtained ADD and ADHD subtype clusters did also not differ regarding these variables (cf. Table 1). This suggests that the dynamics of pro-active and inhibitory control processes in the theta frequency band may provide a clinically relevant tool to substantiate the diagnostic categorization of AD(H)D subtypes, the validity of which has been critically discussed (Vahid et al., 2019; Willcutt et al., 2012). At present, the standard diagnostic procedure to distinguish AD(H)D subtypes is based on clinical interviews and questionnaires completed by different raters. The current results suggest that the analysis of neural dynamics underlying pro-active control and inhibitory control processes may prove useful for clinical diagnostic procedures in the future. Along these lines, it may in the future be interesting to further examine this using machine learning approaches (Itani et al., 2019; Müller et al., 2020; Vahid et al., 2019) and to investigate whether the dynamics between pro-active and inhibitory control may provide a metric for a reliable classification of AD(H)D subtypes on an individual level in clinical settings.

For the obtained clustering, it is particularly the strong pre-trial theta activity that distinguishes patients with ADD from those with ADHD. Corroborating previous findings (Bluschke et al., 2016b), patients within the ADD-cluster committed fewer response inhibition errors than those within the ADHD-cluster. Although this may suggest that particularly the pre-trial theta band activity and hence pro-active control processes are important for successful response inhibition performance in AD(H)D subgroups, the pattern is actually more complex: The reason is that the control group showed the best response inhibition

Table 3
Correlation of mean pretrial-/within-trial correlations with false alarm rates.

Group	Corr(ptTBA, wtTBA) Go trials	Nogo trials
Control	**$r = 0.517^{***}$; $p < 0.001$**	**–**
ADD	–	–
ADD cluster	–	–
ADHD	–	$r = 0.429^{*}$; $p = 0.046$
ADHD cluster	–	$r = 0.448^{**}$; $p = 0.019$

pre-trial theta-band activity (ptTBA); within-trial theta-band activity (wtTBA)

performance while at the same time displaying weaker pre-trial theta band activity than the ADD-cluster. As also the ADHD-cluster did not differ from controls in pre-trial theta band activity (see Fig. 4), it cannot only be the strength of pro-active control-related theta band activity alone that affects performance. Rather, the inter-relation of ptTBA and wtTBA for response inhibition performance is important to consider. This is evidenced by the analyses presented in Table 3. In the ADD-cluster, the inter-relation between ptTBA and wtTBA was not associated with performance. It seems that it is the combination of these factors that affects response inhibition performance and differentiates between ADD-cluster and the ADHD-cluster. The stronger ptTBA and presumably stronger proactive control processes in the ADD-cluster explains the better inhibitory control performance compared to patients within the ADHD-cluster. A negative influence of the ptTBA-wtTBA correlation on response inhibition seems to occur especially when ptTBA and proactive control are low in the first place (i.e. in the ADHD group). This suggests that the strength of ptTBA may be most important for behavioural performance in response inhibition and that a high level of ptTBA can eliminate or compensate otherwise negative effects of a strong inter-relation of ptTBA and wtTBA on inhibitory control.

However, why then does the control group show the best response inhibition performance even though ptTBA and wtTBA were not inter-related and ptTBA was as low as in the ADHD-cluster? The explanation may lie in the different functional neuroanatomical regions that were associated with ptTBA in controls and AD(H)D patients. In the control group, ptTBA was associated with the right inferior frontal gyrus (rIFG, BA45), which is well-known to play a role in inhibitory control processes (Aron et al., 2004; Bari and Robbins, 2013). It appears that the relatively low rIFG theta activity in the pre-trial interval of controls is sufficient to provide the necessary level of inhibitory control. To the extent that inhibitory processes in the control group are “anticipated” in the pre-trial interval in the rIFG (an essential aspect of pro-active control), inhibitory activity during the trial is less crucial for good response inhibition performance. This may explain the lack of a correlation between ptTBA and wtTBA in controls who still were able to achieve good inhibition performance. Opposed to the control group, the ptTBA in patients with AD(H)D patients was associated with right middle frontal regions (BA10). This region, however, has not consistently been described to be part of the cortical response inhibition network (Bari and Robbins, 2013). Since patients within the ADHD-cluster seemingly involve a different brain region in the pre-trial interval that is less relevant for inhibitory control, the dynamics described above cannot develop as it is the in controls. It is possible that in addition to the complex effects of the factors “strength of ptTBA” and “inter-relation of ptTBA and wtTBA”, the functional neuroanatomical region active during ptTBA is a third important factor underlying the ability to inhibit prepotent responses. Likely, it is the complex interplay of these factors underlying inhibitory control and its modulation in AD(H)D subtypes. This multi-factorial pattern is captured by AD(H)D subtype symptom clusters.

At this point, it has to be acknowledged that the captured pattern was reflected using a well-motivated, yet specific methodological approach (cf. introduction). One can think about different methodological approaches, e.g. using entropy-based measures, or other more complex measures of oscillatory dynamics such as cross-frequency coupling (Cohen, 2014b). The latter may be relevant since also beta frequency oscillations have been shown to play a role in response inhibition and the combination of theta and beta frequency oscillatory regimes is targeted in neurofeedback treatments in AD(H)D (Bluschke et al., 2016c; Enriquez-Geppert et al., 2019). Furthermore, source reconstruction points to multiple distinct source activations, for example elevated ptTBA in the precuneus in the AD(H)D group (see Fig. 2), which may suggest that also differences in top-down attentional allocation (Shomstein, 2012) contribute to the pattern of effects. Importantly, we do not state that the analyzed regions (see Table 2) in this work are solely responsible for the observed sub-diagnostic distinction. While we restricted our analyses to the location of maximum activation (located in frontal regions) in order to rely our interpretation on the strongest results, future studies might investigate possible network effects spanning multiple areas. This could further help enhance the separability of ADD and ADHD based on neurophysiological indices. A possible methodological limitation lies within varying trial numbers included in the analyses between diagnostic groups. Although care has been taken to provide sufficient numbers of trials for each condition and participant for statistical analysis, it cannot be completely ruled out that conditions and groups differ with regards to outlier sensitivity and/or signal-to-noise ratio (Cohen, 2017). This possible limitation necessarily results from a trade-off between data quantity (as reflected in the duration of the experimental session) and confounding time-related factors such as increasing fatigue and/or decreasing focus. Still, distinct sources were identified via beamforming theta oscillations, which were shown to be task relevant theoretically (see Introduction) and in this sample (Fig. 2). The observation that sources differ between clustered AD(H)D subgroups might gain clinical relevance with more investigations of pre-trial activity in AD(H)D. It is not yet clear why patients do not recruit precisely those anatomical regions that have been previously reported to be relevant for response inhibition in healthy controls such as rIFG. However, this study provides a first step for an understanding of this issue, by systematically comparing theta activity in pre-trial and within-trial phases. To obtain a high signal-to-noise ratio in the data, only correct trials were taken into account. The results may therefore, also be interpreted that patients within the estimated AD(H)D-clusters arrive at the correct behavioral responses in a different way. Future studies may further examine the investigated pre-trial/within-trial dynamics when response inhibition was not successful.

In summary, the study reveals a novel facet of neural mechanisms underlying AD(H)D subtype-specific differences during inhibitory control and impulsive behaviour. We show that the dynamics between pre-trial (pro-active) and within-trial (inhibition-related) control processes, as reflected by theta frequency oscillations, allows to cluster AD(H)D subtypes. This clustering seems to be robust and not affected by various clinically relevant parameters. We show that response inhibition, and its differential modulation in AD(H)D subtypes, depends on the complex interplay of (at least) three factors: (i) strength of pro-active control-related theta-band activity, (ii) the inter-relation of pro-active control and inhibition-relation theta band activity and (iii) the functional neuroanatomical region active during theta-related pro-active control processes. The results reveal novel neurophysiological facets of AD(H)D.

CRediT authorship contribution statement

Nico Adelhöfer: Conceptualization, Data curation, Formal analysis, Investigation, Methodology, Software, Validation, Visualization, Writing - original draft, Writing - review & editing. **Annet Bluschke:** Conceptualization, Investigation, Methodology, Validation, Visualization, Writing - original draft, Writing - review & editing. **Veit Roessner:** Funding acquisition, Resources, Writing - review & editing. **Christian Beste:** Conceptualization, Funding acquisition, Methodology, Project administration, Resources, Supervision, Validation, Writing - original draft, Writing - review & editing.

Declaration of Competing Interest

The authors declare that they have no known competing financial interests or personal relationships that could have appeared to influence the work reported in this paper.

Acknowledgements

We thank all participants and patients taking part in the study. This work was supported by a Grant from the Deutsche

Forschungsgemeinschaft (DFG) SFB 940 project B8 and partly by FOR 2698 to CB.

Appendix A. Supplementary data

Supplementary data to this article can be found online at https://doi.org/10.1016/j.nicl.2021.102609.

References

Adelhöfer, N., Beste, C., 2020. Pre-trial theta band activity in the ventromedial prefrontal cortex correlates with inhibition-related theta band activity in the right inferior frontal cortex. Neuroimage 219, 117052. https://doi.org/10.1016/j.neuroimage.2020.117052.

Adelhöfer, N., Beste, C., 2019. Validity expectancies shape the interplay of cueing and task demands during inhibitory control associated with right inferior frontal regions. Brain Struct. Funct. 224 (5), 1911–1924. https://doi.org/10.1007/s00429-019-01884-y.

Adelhöfer, N., Gohil, K., Passow, S., Teufert, B., Roessner, V., Li, S.-C., Beste, C., 2018. The system-neurophysiological basis for how methylphenidate modulates perceptual-attentional conflicts during auditory processing. Hum. Brain Mapp. 39 (12), 5050–5061. https://doi.org/10.1002/hbm.v39.1210.1002/hbm.24344.

Adelhöfer, N., Mückschel, M., Teufert, B., Ziemssen, T., Beste, C., 2019. Anodal tDCS affects neuromodulatory effects of the norepinephrine system on superior frontal theta activity during response inhibition. Brain Struct. Funct. 224 (3), 1291–1300. https://doi.org/10.1007/s00429-019-01839-3.

Ahmadi, N., Mohammadi, M.R., Araghi, S.M., Zarafshan, H., 2014. Neurocognitive Profile of Children with Attention Deficit Hyperactivity Disorders (ADHD): A comparison between subtypes. Iran J. Psychiatry 9, 197–202.

Albajara Sáenz, A., Villemonteix, T., Massat, I., 2019. Structural and functional neuroimaging in attention-deficit/hyperactivity disorder. Dev. Med. Child Neurol. 61 (4), 399–405. https://doi.org/10.1111/dmcn.2019.61.issue-410.1111/dmcn.14050.

Albrecht, B., Brandeis, D., von Sandersleben, H., Valko, L., Heinrich, H., Xu, X., Drechsler, R., Heise, A., Kuntsi, J., Müller, U.C., Asherson, P., Steinhausen, H.-C., Rothenberger, A., Banaschewski, T., 2014. Genetics of preparation and response control in ADHD: the role of DRD4 and DAT1. J. Child Psychol. Psychiatry 55 (8), 914–923. https://doi.org/10.1111/jcpp.12212.

Aldemir, R., Demirci, E., Per, H., Canpolat, M., Özmen, S., Tokmakçı, M., 2018. Investigation of attention deficit hyperactivity disorder (ADHD) sub-types in children via EEG frequency domain analysis. Int. J. Neurosci. 128 (4), 349–360. https://doi.org/10.1080/00207454.2017.1382493.

Aron, A.R., Robbins, T.W., Poldrack, R.A., 2004. Inhibition and the right inferior frontal cortex. Trends Cogn. Sci. (Regul. Ed.) 8 (4), 170–177. https://doi.org/10.1016/j.tics.2004.02.010.

Baijot, S., Cevallos, C., Zarka, D., Leroy, A., Slama, H., Colin, C., Deconinck, N., Dan, B., Cheron, G., 2017. EEG Dynamics of a Go/Nogo Task in Children with ADHD. Brain Sci. 7 (12), 167. https://doi.org/10.3390/brainsci7120167.

Bari, A., Robbins, T.W., 2013. Inhibition and impulsivity: behavioral and neural basis of response control. Prog. Neurobiol. 108, 44–79. https://doi.org/10.1016/j.pneurobio.2013.06.005.

Beste, C., Ness, V., Falkenstein, M., Saft, C., 2011. On the role of fronto-striatal neural synchronization processes for response inhibition—Evidence from ERP phase-synchronization analyses in pre-manifest Huntington's disease gene mutation carriers. Neuropsychologia 49 (12), 3484–3493. https://doi.org/10.1016/j.neuropsychologia.2011.08.024.

Bluschke, A., Broschwitz, F., Kohl, S., Roessner, V., Beste, C., 2016a. The neuronal mechanisms underlying improvement of impulsivity in ADHD by theta/beta neurofeedback. Sci. Rep. 6, 31178. https://doi.org/10.1038/srep31178.

Bluschke, A., Friedrich, J., Schreiter, M.L., Roessner, V., Beste, C., 2018. A comparative study on the neurophysiological mechanisms underlying effects of methylphenidate and neurofeedback on inhibitory control in attention deficit hyperactivity disorder. Neuroimage Clin. 20, 1191–1203. https://doi.org/10.1016/j.nicl.2018.10.027.

Bluschke, A., Roessner, V., Beste, C., 2016b. Specific cognitive-neurophysiological processes predict impulsivity in the childhood attention-deficit/hyperactivity disorder combined subtype. Psychol. Med. 46 (6), 1277–1287. https://doi.org/10.1017/S0033291715002822.

Bluschke, A., Roessner, V., Beste, C., 2016c. Editorial Perspective: How to optimise frequency band neurofeedback for ADHD. J, Child Psychol. Psychiatry 57, 457–461. https://doi.org/10.1111/jcpp.12521.

Bluschke, A., Schreiter, M.L., Friedrich, J., Adelhöfer, N., Roessner, V., Beste, C., 2020. Neurofeedback trains a superordinate system relevant for seemingly opposing behavioral control deficits depending on ADHD subtype. Dev Sci e12956. https://doi.org/10.1111/desc.12956.

Braver, T.S., 2012. The variable nature of cognitive control: a dual mechanisms framework. Trends Cogn. Sci. (Regul.) 16 (2), 106–113. https://doi.org/10.1016/j.tics.2011.12.010.

Cavanagh, J.F., Frank, M.J., 2014. Frontal theta as a mechanism for cognitive control. Trends Cogn. Sci. (Regul.) 18 (8), 414–421. https://doi.org/10.1016/j.tics.2014.04.012.

Chmielewski, W.X., Mückschel, M., Dippel, G., Beste, C., 2016. Concurrent information affects response inhibition processes via the modulation of theta oscillations in cognitive control networks. Brain Struct Funct 221 (8), 3949–3961. https://doi.org/10.1007/s00429-015-1137-1.

Chmielewski, W.X., Mückschel, M., Stock, A.-K., Beste, C., 2015. The impact of mental workload on inhibitory control subprocesses. Neuroimage 112, 96–104. https://doi.org/10.1016/j.neuroimage.2015.02.060.

Chmielewski, W.X., Tiedt, A., Bluschke, A., Dippel, G., Roessner, V., Beste, C., 2018. Effects of multisensory stimuli on inhibitory control in adolescent ADHD: It is the content of information that matters. Neuroimage Clin 19, 527–537. https://doi.org/10.1016/j.nicl.2018.05.019.

Cohen, M.X., 2017. Rigor and replication in time-frequency analyses of cognitive electrophysiology data. Int. J. Psychophysiol. 111, 80–87. https://doi.org/10.1016/j.ijpsycho.2016.02.001.

Cohen, M.X., 2014a. A neural microcircuit for cognitive conflict detection and signaling. Trends Neurosci. 37 (9), 480–490. https://doi.org/10.1016/j.tins.2014.06.004.

Cohen, M.X., 2014b. Analyzing neural time series data: theory and practice, Issues in clinical and cognitive neuropsychology. The MIT Press, Cambridge, Massachusetts.

Cooper, P.S., Wong, A.S.W., Fulham, W.R., Thienel, R., Mansfield, E., Michie, P.T., Karayanidis, F., 2015. Theta frontoparietal connectivity associated with proactive and reactive cognitive control processes. Neuroimage 108, 354–363. https://doi.org/10.1016/j.neuroimage.2014.12.028.

Cooper, P.S., Wong, A.S.W., McKewen, M., Michie, P.T., Karayanidis, F., 2017. Frontoparietal theta oscillations during proactive control are associated with goal-updating and reduced behavioral variability. Biol. Psychol. 129, 253–264. https://doi.org/10.1016/j.biopsycho.2017.09.008.

Cunillera, T., Fuentemilla, L., Periañez, J., Marco-Pallarès, J., Krämer, U.M., Càmara, E., Münte, T.F., Rodríguez-Fornells, A., 2012. Brain oscillatory activity associated with task switching and feedback processing. Cogn. Affect Behav. Neurosci. 12 (1), 16–33. https://doi.org/10.3758/s13415-011-0075-5.

De Blasio, F.M., Barry, R.J., 2013. Prestimulus delta and theta determinants of ERP responses in the Go/NoGo task. Int. J. Psychophysiol. 87 (3), 279–288. https://doi.org/10.1016/j.ijpsycho.2012.09.016.

Diamond, A., 2013. Executive functions. Annu. Rev. Psychol. 64 (1), 135–168. https://doi.org/10.1146/annurev-psych-113011-143750.

Dippel, G., Chmielewski, W., Mückschel, M., Beste, C., 2016. Response mode-dependent differences in neurofunctional networks during response inhibition: an EEG-beamforming study. Brain Struct. Funct. 221 (8), 4091–4101. https://doi.org/10.1007/s00429-015-1148-y.

Dippel, G., Mückschel, M., Ziemssen, T., Beste, C., 2017. Demands on response inhibition processes determine modulations of theta band activity in superior frontal areas and correlations with pupillometry - Implications for the norepinephrine system during inhibitory control. Neuroimage 157, 575–585. https://doi.org/10.1016/j.neuroimage.2017.06.037.

Doehnert, M., Brandeis, D., Schneider, G., Drechsler, R., Steinhausen, H.-C., 2013. A neurophysiological marker of impaired preparation in an 11-year follow-up study of attention-deficit/hyperactivity disorder (ADHD). J Child Psychol Psychiatry 54, 260–270. https://doi.org/10.1111/j.1469-7610.2012.02572.x.

Döpfner, M., Lehmkuhl, G., Görtz-Dorten, A., Breuer, D., Lehmkuhl, G., Görtz-Dorten, A., 2008. DISYPS-II: Diagnostik-System für psychische Störungen nach ICD-10 und DSM-IV für Kinder und Jugendliche-II. Huber, Hogrefe Testverl.

Enriquez-Geppert, S., Smit, D., Pimenta, M.G., Arns, M., 2019. Neurofeedback as a Treatment Intervention in ADHD: Current Evidence and Practice. Curr Psychiatry Rep 21, 46. https://doi.org/10.1007/s11920-019-1021-4.

Fallgatter, A.J., Ehlis, A.-C., Rösler, M., Strik, W.K., Blocher, D., Herrmann, M.J., 2005. Diminished prefrontal brain function in adults with psychopathology in childhood related to attention deficit hyperactivity disorder. Psychiatry Res 138 (2), 157–169. https://doi.org/10.1016/j.pscychresns.2004.12.002.

Fallgatter, A.J., Ehlis, A.-C., Seifert, J., Strik, W.K., Scheuerpflug, P., Zillessen, K.E., Herrmann, M.J., Warnke, A., 2004. Altered response control and anterior cingulate function in attention-deficit/hyperactivity disorder boys. Clin Neurophysiol 115 (4), 973–981. https://doi.org/10.1016/j.clinph.2003.11.036.

Gayen, A.K., 1951. The Frequency Distribution of the Product-Moment Correlation Coefficient in Random Samples of Any Size Drawn from Non-Normal Universes. Biometrika 38 (1/2), 219. https://doi.org/10.2307/2332329.

Gross, J., Kujala, J., Hamalainen, M., Timmermann, L., Schnitzler, A., Salmelin, R., 2001. Dynamic imaging of coherent sources: Studying neural interactions in the human brain. Proc. Natl. Acad. Sci. U.S.A. 98 (2), 694–699. https://doi.org/10.1073/pnas.98.2.694.

Halder, T., Talwar, S., Jaiswal, A.K., Banerjee, A., 2019. Quantitative Evaluation in Estimating Sources Underlying Brain Oscillations Using Current Source Density Methods and Beamformer Approaches. eNeuro 6, ENEURO.0170-19.2019. https://doi.org/10.1523/ENEURO.0170-19.2019.

Handy, T.C. (Ed.), 2009. Brain signal analysis: advances in neuroelectric and neuromagnetic methods. The MIT Press, Cambridge, MA.

Hong, X., Sun, J., Wang, J., Li, C., Tong, S., 2020. Attention-related modulation of frontal midline theta oscillations in cingulate cortex during a spatial cueing Go/NoGo task. Int. J. Psychophysiol. 148, 1–12. https://doi.org/10.1016/j.ijpsycho.2019.11.011.

Hong, X., Wang, Y., Sun, J., Li, C., Tong, S., 2017. Segregating Top-Down Selective Attention from Response Inhibition in a Spatial Cueing Go/NoGo Task: An ERP and Source Localization Study. Sci Rep 7, 9662. https://doi.org/10.1038/s41598-017-08807-z.

Hsieh, L.-T., Ranganath, C., 2014. Frontal midline theta oscillations during working memory maintenance and episodic encoding and retrieval. Neuroimage 85 (Pt 2), 721–729. https://doi.org/10.1016/j.neuroimage.2013.08.003.

Huster, R.J., Enriquez-Geppert, S., Lavallee, C.F., Falkenstein, M., Herrmann, C.S., 2013. Electroencephalography of response inhibition tasks: functional networks and

cognitive contributions. Int. J. Psychophysiol. 87 (3), 217–233. https://doi.org/10.1016/j.ijpsycho.2012.08.001.
Isabella, S., Ferrari, P., Jobst, C., Cheyne, J.A., Cheyne, D., 2015. Complementary roles of cortical oscillations in automatic and controlled processing during rapid serial tasks. NeuroImage 118, 268–281. https://doi.org/10.1016/j.neuroimage.2015.05.081.
Itani, S., Rossignol, M., Lecron, F., Fortemps, P., Stoean, R., 2019. Towards interpretable machine learning models for diagnosis aid: A case study on attention deficit/hyperactivity disorder. PLoS ONE 14 (4), e0215720. https://doi.org/10.1371/journal.pone.0215720.
Jensen, O., 2006. Maintenance of multiple working memory items by temporal segmentation. Neuroscience 139 (1), 237–249. https://doi.org/10.1016/j.neuroscience:2005.06.004.
Johannes, T., 2020. 3D visualization of GMM learning via the EM algorithm.
Johnstone, S.J., Barry, R.J., Markovska, V., Dimoska, A., Clarke, A.R., 2009. Response inhibition and interference control in children with AD/HD: a visual ERP investigation. Int. J. Psychophysiol. 72 (2), 145–153. https://doi.org/10.1016/j.ijpsycho.2008.11.007.
Kenemans, J.L., Bekker, E.M., Lijffijt, M., Overtoom, C.C.E., Jonkman, L.M., Verbaten, M. N., 2005. Attention deficit and impulsivity: selecting, shifting, and stopping. Int. J. Psychophysiol. 58 (1), 59–70. https://doi.org/10.1016/j.ijpsycho.2005.03.009.
Kolodny, T., Mevorach, C., Stern, P., Biderman, N., Ankaoua, M., Tsafrir, S., Shalev, L., 2020. Fronto-parietal engagement in response inhibition is inversely scaled with attention-deficit/hyperactivity disorder symptom severity. Neuroimage Clin 25, 102119. https://doi.org/10.1016/j.nicl.2019.102119.
Liebrand, M., Pein, I., Tzvi, E., Krämer, U.M., 2017. Temporal Dynamics of Proactive and Reactive Motor Inhibition. Front Hum Neurosci 11, 204. https://doi.org/10.3389/fnhum.2017.00204.
Maris, E., Oostenveld, R., 2007. Nonparametric statistical testing of EEG- and MEG-data. J. Neurosci. Methods 164 (1), 177–190. https://doi.org/10.1016/j.jneumeth.2007.03.024.
Metin, B., Roeyers, H., Wiersema, J.R., van der Meere, J., Sonuga-Barke, E., 2012. A meta-analytic study of event rate effects on Go/No-Go performance in attention-deficit/hyperactivity disorder. Biol. Psychiatry 72 (12), 990–996. https://doi.org/10.1016/j.biopsych.2012.08.023.
Miller, J., Patterson, T., Ulrich, R., 1998. Jackknife-based method for measuring LRP onset latency differences. Psychophysiology 35 (1), 99–115.
Miyake, A., Friedman, N.P., Emerson, M.J., Witzki, A.H., Howerter, A., Wager, T.D., 2000. The unity and diversity of executive functions and their contributions to complex "Frontal Lobe" tasks: a latent variable analysis. Cogn Psychol 41 (1), 49–100. https://doi.org/10.1006/cogp.1999.0734.
Müller, A., Vetsch, S., Pershin, I., Candrian, G., Baschera, G.-M., Kropotov, J.D., Kasper, J., Rehim, H.A., Eich, D., 2020. EEG/ERP-based biomarker/neuroalgorithms in adults with ADHD: Development, reliability, and application in clinical practice. World J. Biol. Psychiatry 21 (3), 172–182. https://doi.org/10.1080/15622975.2019.1605198.
Nigbur, R., Ivanova, G., Stürmer, B., 2011. Theta power as a marker for cognitive interference. Clin Neurophysiol 122 (11), 2185–2194. https://doi.org/10.1016/j.clinph.2011.03.030.
Oostenveld, R., Stegeman, D.F., Praamstra, P., van Oosterom, A., 2003. Brain symmetry and topographic analysis of lateralized event-related potentials. Clin. Neurophysiol. 114 (7), 1194–1202. https://doi.org/10.1016/S1388-2457(03)00059-2.
Paul-Jordanov, I., Bechtold, M., Gawrilow, C., 2010. Methylphenidate and if-then plans are comparable in modulating the P300 and increasing response inhibition in children with ADHD. Atten Defic Hyperact Disord 2 (3), 115–126. https://doi.org/10.1007/s12402-010-0028-9.
Pertermann, M., Bluschke, A., Roessner, V., Beste, C., 2019. The Modulation of Neural Noise Underlies the Effectiveness of Methylphenidate Treatment in Attention-Deficit/Hyperactivity Disorder. Biol Psychiatry Cogn Neurosci Neuroimaging 4 (8), 743–750. https://doi.org/10.1016/j.bpsc.2019.03.011.
Pievsky, M.A., McGrath, R.E., 2018. The Neurocognitive Profile of Attention-Deficit/Hyperactivity Disorder: A Review of Meta-Analyses. Arch Clin Neuropsychol 33, 143–157. https://doi.org/10.1093/arclin/acx055.
Pliszka, S.R., Liotti, M., Bailey, B.Y., Perez 3rd, R., Glahn, D., Semrud-Clikeman, M., 2007. Electrophysiological effects of stimulant treatment on inhibitory control in children with attention-deficit/hyperactivity disorder. J Child Adolesc Psychopharmacol 17, 356–366. https://doi.org/10.1089/cap.2006.0081.
Pscherer, C., Mückschel, M., Summerer, L., Bluschke, A., Beste, C., 2019. On the relevance of EEG resting theta activity for the neurophysiological dynamics underlying motor inhibitory control. Hum Brain Mapp 40 (14), 4253–4265. https://doi.org/10.1002/hbm.v40.1410.1002/hbm.24699.
Quetscher, C., Yildiz, A., Dharmadhikari, S., Glaubitz, B., Schmidt-Wilcke, T., Dydak, U., Beste, C., 2015. Striatal GABA-MRS predicts response inhibition performance and its cortical electrophysiological correlates. Brain Struct Funct 220 (6), 3555–3564. https://doi.org/10.1007/s00429-014-0873-y.
Randall, K.D., Brocki, K.C., Kerns, K.A., 2009. Cognitive control in children with ADHD-C: how efficient are they? Child Neuropsychol 15 (2), 163–178. https://doi.org/10.1080/09297040802464148.
Randall, W.M., Smith, J.L., 2011. Conflict and inhibition in the cued-Go/NoGo task. Clin Neurophysiol 122 (12), 2400–2407. https://doi.org/10.1016/j.clinph.2011.05.012.
Seifert, J., Scheuerpflug, P., Zillessen, K.-E., Fallgatter, A., Warnke, A., 2003. Electrophysiological investigation of the effectiveness of methylphenidate in children with and without ADHD. J Neural Transm 110 (7), 821–829. https://doi.org/10.1007/s00702-003-0818-8.
Shomstein, S., 2012. Cognitive functions of the posterior parietal cortex: top-down and bottom-up attentional control. Front. Integr. Neurosci. 6 https://doi.org/10.3389/fnint.2012.00038.
Smith, J.L., Johnstone, S.J., Barry, R.J., 2007. Response priming in the Go/NoGo task: the N2 reflects neither inhibition nor conflict. Clin Neurophysiol 118 (2), 343–355. https://doi.org/10.1016/j.clinph.2006.09.027.
Smith, J.L., Johnstone, S.J., Barry, R.J., 2006. Effects of pre-stimulus processing on subsequent events in a warned Go/NoGo paradigm: response preparation, execution and inhibition. Int. J. Psychophysiol. 61 (2), 121–133. https://doi.org/10.1016/j.ijpsycho.2005.07.013.
Smith, J.L., Johnstone, S.J., Barry, R.J., 2004. Inhibitory processing during the Go/NoGo task: an ERP analysis of children with attention-deficit/hyperactivity disorder. Clin Neurophysiol 115 (6), 1320–1331. https://doi.org/10.1016/j.clinph.2003.12.027.
Uddin, L.Q., Dajani, D.R., Voorhies, W., Bednarz, H., Kana, R.K., 2017. Progress and roadblocks in the search for brain-based biomarkers of autism and attention-deficit/hyperactivity disorder. Transl Psychiatry 7, e1218. https://doi.org/10.1038/tp.2017.164.
Ulrich, R., Miller, J., 2001. Using the jackknife-based scoring method for measuring LRP onset effects in factorial designs. Psychophysiology 38 (5), 816–827.
Vahid, A., Bluschke, A., Roessner, V., Stober, S., Beste, C., 2019. Deep Learning Based on Event-Related EEG Differentiates Children with ADHD from Healthy Controls. J Clin Med 8 (7), 1055. https://doi.org/10.3390/jcm8071055.
van Driel, J., Swart, J.C., Egner, T., Ridderinkhof, K.R., Cohen, M.X., 2015. (No) time for control: Frontal theta dynamics reveal the cost of temporally guided conflict anticipation. Cogn Affect Behav Neurosci 15 (4), 787–807. https://doi.org/10.3758/s13415-015-0367-2.
Van Veen, B.D., van Drongelen, W., Yuchtman, M., Suzuki, A., 1997. Localization of brain electrical activity via linearly constrained minimum variance spatial filtering. IEEE Trans Biomed Eng 44, 867–880. https://doi.org/10.1109/10.623056.
Vuillier, L., Bryce, D., Szücs, D., Whitebread, D., Wan, X., 2016. The Maturation of Interference Suppression and Response Inhibition: ERP Analysis of a Cued Go/Nogo Task. PLoS ONE 11 (11), e0165697. https://doi.org/10.1371/journal.pone.0165697.
Waldmann, H.-C., 2008. German WISC-IV short forms: a scenario-based evaluation of statistical properties. Diagnostica 54, 202–210.
Willcutt, E.G., Nigg, J.T., Pennington, B.F., Solanto, M.V., Rohde, L.A., Tannock, R., Loo, S.K., Carlson, C.L., McBurnett, K., Lahey, B.B., 2012. Validity of DSM-IV attention deficit/hyperactivity disorder symptom dimensions and subtypes. J Abnorm Psychol 121, 991–1010. https://doi.org/10.1037/a0027347.
Yamanaka, K., Yamamoto, Y., 2010. Single-trial EEG power and phase dynamics associated with voluntary response inhibition. J Cogn Neurosci 22, 714–727. https://doi.org/10.1162/jocn.2009.21258.
Yordanova, J., Kolev, V., Rothenberger, A., 2013. Event-related oscillations reflect functional asymmetry in children with attention deficit/hyperactivity disorder. Suppl Clin Neurophysiol 62, 289–301. https://doi.org/10.1016/b978-0-7020-5307-8.00018-1.
Zavala, B., Jang, A., Trotta, M., Lungu, C.I., Brown, P., Zaghloul, K.A., 2018. Cognitive control involves theta power within trials and beta power across trials in the prefrontal-subthalamic network. Brain 141, 3361–3376. https://doi.org/10.1093/brain/awy266.